Åbo Akademi

OPEN ACCESS

This is an electronic reprint of the original article. This reprint may differ from the original in pagination and typographic detail.

Electrospinning of Electroconductive Water-Resistant Nanofibers of PEDOTPSS, Cellulose Nanofibrils and PEO: Fabrication Characterization, and Cytocompatibility

Latonen, Rose-Marie; Wrzosek Cabrera, Jose Antonio; Lund, Sara; Kosourov, Sergey; Vajravel, Sindhujaa; Boeva, Zhanna; Wang, Xiaoju; Xu, Chunlin; Allahverdiyeva, Yagut

Published in:
ACS Applied Bio Materials

DOI:
10.1021/acsabm.0c00989

Published: 01/01/2020

Document Version
Accepted author manuscript

Document License
All rights reserved

Link to publication

Please cite the original version:
Latonen, R.-M., Wrzosek Cabrera, J. A., Lund, S., Kosourov, S., Vajravel, S., Boeva, Z., Wang, X., Xu, C., & Allahverdiyeva, Y. (2020). Electrospinning of Electroconductive Water-Resistant Nanofibers of PEDOTPSS, Cellulose Nanofibrils and PEO: Fabrication Characterization, and Cytocompatibility. *ACS Applied Bio Materials*, *4*(1), 483-493. https://doi.org/10.1021/acsabm.0c00989

General rights
Copyright and moral rights for the publications made accessible in the public portal are retained by the authors and/or other copyright owners and it is a condition of accessing publications that users recognise and abide by the legal requirements associated with these rights.

Take down policy
If you believe that this document breaches copyright please contact us providing details, and we will remove access to the work immediately and investigate your claim.

This document is downloaded from the Research Information Portal of ÅAU: 20. Apr. 2024

Electrospinning of electroconductive water-resistant nanofibers of PEDOT-PSS, cellulose nanofibrils and PEO: fabrication, characterization and cytocompatibility

Rose-Marie Latonen*[,†], Jose Antonio Wrzosek Cabrera[†], Sara Lund[†], Sergey Kosourov[‡], Sindhujaa Vajravel[‡], Zhanna Boeva[†], Xiaoju Wang[§], Chunlin Xu[§], Yagut Allahverdiyeva[‡]

[†]Johan Gadolin Process Chemistry Centre, Laboratory of Molecular Science and Engineering, Åbo Akademi University, Biskopsgatan 8, FI-20500 Turku/Åbo, Finland

[‡]Molecular Plant Biology, Department of Biochemistry, University of Turku, FI-20014 Turku, Finland

[§]Johan Gadolin Process Chemistry Centre, Laboratory of Natural Materials Technology, Åbo Akademi University, Porthansgatan 3, FI-20500 Turku/Åbo, Finland

KEYWORDS Electrospinning, cellulose nanofibrils, poly(3,4-ethylenedioxythiophene), poly(ethylene oxide), nanofiber, composite, cyclic voltammetry, biocompatibility

ABSTRACT Electrically conductive composite nanofibers were fabricated using poly(3,4-ethylenedioxythiophene) doped with poly(styrenesulfonate) (PEDOT-PSS) and cellulose nanofibrils (CNFs) via the electrospinning technique. Poly(ethylene oxide) (PEO) was used to

assist the electrospinning process, and poly(ethylene glycol) diglycidyl ether was used to induce chemical crosslinking, enabling stability of the formed fibrous mats in water. The experimental parameters regarding the electrospinning polymer dispersion and electrospinning process were carefully studied to achieve a reproducible method to obtain bead-free nanofibrous mats with high stability after water contact, with an electrical conductivity of 13 ± 5 S m^{-1}, thus making them suitable for bioelectrochemical applications. The morphology of the electrospun nanofibers was characterized by scanning electron microscopy, and the C/S ratio was determined with energy dispersive X-ray analysis. Cyclic voltammetric studies showed that the PEDOT-PSS/CNF/PEO composite fibers exhibited high electroactivity and high stability in water for at least two months. By infrared spectroscopy, the slightly modified fiber morphology after water contact was demonstrated to be due to dissolution of some part of the PEO in the fiber structure. The biocompatibility of the PEDOT-PSS/CNF/PEO composite fibers when used as an electroconductive substrate to immobilize microalgae and cyanobacteria in a photosynthetic bioelectrochemical cell was also demonstrated.

1. INTRODUCTION

Electrospinning is a fascinating, simple and versatile fiber fabrication technique allowing for the production of a variety of polymeric fibers with different diameters in dry form. Electrospun polymeric mats also possess advantages, such as a high surface-to-volume ratio, tunable porosity, the possibility of forming a wide variety of shapes and sizes and the ability to control their composition to achieve the desired properties and functionalities. Therefore, their application fields can vary from nanocatalysis, tissue engineering, medical dressing, filtration, optical and chemical sensors and electrode materials to cell growth cultures. Electrospinning of a variety of

"green" polymers such as polylactic acid, polyurethanes, hyaluronic acid, silk fibroin, collagen, starch and cellulose has gained much interest due to their biocompatibility and biodegradability and their suitability in the aforementioned application fields.[1,2] Recently, nanocellulose, both as cellulose nanofibrils (CNFs) and cellulose nanocrystals (CNCs), has also been incorporated into polymer dispersions for electrospinning. Nanocellulose has been used to enhance the mechanical properties[3-6] and reduce the oxygen permeability[7] of nonwoven fibrous mats, to increase the use of renewable, abundant and inexpensive natural resources for industrial filter production[8,9], to decrease the water solubility of electrospun poly(vinyl alcohol) (PVA) nanofibrous mats[9], and to enhance the water retention capacity of poly(ε-captolactone) fibers,[6] and it has also been used as a stabilization agent.[4]

Carbon nanotubes have widely been used to endow nonwoven fibrous mats with electrical conductivity, enhanced surface area and porosity.[4,10] In addition, electrically conducting polymers (ECPs) in the form of nanofibrous structures offer many useful features for several application fields. For example, polyaniline has been electrospun to develop stretchable and self-healable strain and pressure sensors[11], highly selective and fast responsive dopamine sensors[12] and flexible supercapacitors with a large specific surface area and continuous electroconductive network.[13] Soluble polythiophene-based derivatives have been electrospun for biocompatible tissue engineering materials mimicking the extracellular matrix for electrical cell stimulation.[14] Electrospun biocompatible polypyrrole nanowires modified by covalent attachment of antibodies have been used for immunoglobulin G detection by electrochemical methods in real time.[15] Poly(3,4-ethylenedioxythiophene) (PEDOT) is an attractive ECP due to its high electrical conductivity, good environmental stability, pH insensitivity, medium band gap, low redox potential and transparency in the electrically conducting state.[16] PEDOT has been electrospun as

an EDOT monomer followed by chemical polymerization[17] and as chemically synthesized cylindrical PEDOT particles doped with sodium dodecyl sulfate.[18] PEDOT has also been formed on top of electrospun polyvinylpyrrolidone/Fe(III) p-toluensulfonate oxidant nonwoven mats[19] or on electrospun poly(ethylene terephthalate) fibers spin coated with Fe(III)tosylate by the chemical vapor phase polymerization method.[20] In particular, the cationic form of PEDOT doped with polystyrene sulfonic acid (PSS), which is a water-soluble commercially available ECP, has widely been electrospun to form nanofibrous morphologies for use in different applications. Electrospun PEDOT-PSS has been used as the active semiconducting material between the source and drain in a field effect transistor.[21] Ultrafine PEDOT-PSS nanofibers electrospun with the use of an air flow have been applied as a sensitive ammonia sensor by detecting changes in the current/voltage behavior under different ammonia concentrations.[22] Electrospun fibers of PEDOT-PSS have also been applied as a CO gas sensor by using a quartz crystal microbalance sensing platform[23] and as sensors for inorganic NH_3, HCl and NO_2 gases and various alcohol and water vapors[24] as well as methanol, ethanol, tetrahydrofuran and acetone[25] by the measurement of resistance changes. The thermoresistivity of a polymer film underneath an electrospun PEDOT-PSS fibrous mat has been recorded by the resistance change of PEDOT.[26] A transparent electrospun PEDOT-PSS layer has also been used as a conductive electrode in optoelectronic applications.[27] Furthermore, PEDOT-PSS electrospun nanofibers have been applied as efficient scaffolds for neuronal cell attachment allowing manipulation of the cell morphology[28] and as a swelling-resistant soft electrode material.[29]

Many studies have shown that electrospinning ECPs is challenging due to their rigid structure, low molecular weight, high charge density (because of doping ions) and low viscosity. These are unfavorable rheological properties for producing a uniform dispersion for electrospinning.[12] The

same issues concern nanocellulose; therefore, different flexible polymer carriers are used to facilitate the electrospinning process. Nanocellulose has been electrospun by using a variety of polymer matrices, such as poly(ethylene oxide) (PEO)[3], PVA[4,8,10], starch[5], polyhydroxyalkanoates[7] and poly(lactic acid) (PLA).[30] ECPs, on the other hand, have been electrospun with the aid of poly(vinylpyrrolidone)[10,19,23,25], polyacrylic acid[11,13], poly(methyl methacrylate)[12], poly(lactide-co-glycolic acid)[14], PEO[15,17,21,25,27], PLA[18], poly(ethylene terephthalate)[20] and PVA.[22]

The high volatility, toxicity and high cost of organic solvent systems commonly used within electrospinning applications are drawbacks that one could avoid by using ecofriendly solvents such as water instead. However, when aqueous dispersions containing nanocellulose or PEDOT-PSS are electrospun into nanofibrous mats by the aid of a carrier polymer, the fibers tend to have poor mechanical strength and easily disintegrate and dissolve in contact with water. Several attempts have been made to improve the water resistance of nanofibrous mats. The property of cationic starch to bind with anionic nanocellulose[5] has been used, the addition of a thermocrosslinkable monomer to the polymer dispersion[26] has been applied, chemical crosslinking agents such as (3-glycidyloxypropyl)trimethoxysilane[28] or ethylene glycol diglycidyl ether[31] have been used, a heat-treatment step has been used to improve the bonding between the carrier polymer and PEDOT-PSS[29] and the electrospun fibrous mats have been subjected to glutaraldehyde vapors[32] to induce crosslinking of the fibrous structure.

As discussed above, both nanocellulose and different ECPs have been electrospun separately by the aid of a carrier polymer for various applications. On the other hand, to the best of the authors' knowledge, a combination of nanocellulose, either CNFs or CNCs, and ECPs in an electrospun

fibrous mat has not been studied. A recent study on electrospinning PEDOT-PSS together with chitosan and polyvinyl alcohol for use as an electroconductive cell proliferation scaffold for cardiac tissue engineering is the closest to our work since the structure of chitosan very much resembles that of cellulose.[32] In that study, it was shown that the addition of PEDOT-PSS to fibrous mats mimicking the features of the extracellular matrix imparted electrical conductivity to the fibrous mats and even improved the biocompatibility and cell viability of the scaffolds. Overall, swollen three-dimensional or 3D-printed nanocellulose films and aerogels have shown suitable properties as scaffolds for tissue engineering applications.[33,34]

In the current work, we focused on the preparation and characterization of electrospun composite fibrous mats of PEDOT-PSS, CNF and PEO crosslinked by poly(ethylene glycol) diglycidyl ether (PEGDE) in aqueous solutions. The morphology and elemental composition of the fibers were determined by scanning electron microscopy (SEM) and energy dispersive X-ray analysis (EDXA), respectively. The electroactivity and stability of the fibers were characterized by cyclic voltammetry (CV) in an aqueous electrolyte solution, the chemical structure was studied by FTIR attenuated total reflectance (FTIR-ATR) spectroscopy, and the electrical conductivity was determined by the 4-point probe method. Furthermore, we tested the biocompatibility of these fibrous mats with photosynthetic microbes for suitability as electrode materials for thin-layer immobilization of microalgae and cyanobacteria in a photosynthetic microbial electrochemical cell.

2. EXPERIMENTAL SECTION

2.1. **Materials and chemicals.** Poly(ethylene oxide) (PEO) Mw 600 000 was purchased from Acros Organics and used as a 6 wt% water dispersion. Poly(3,4-

ethylenedioxythiophene)(poly(styrenesulfonate)) (PEDOT-PSS) in water (1.3 %: 0.5 wt% PEDOT, 0.8 wt% PSS) with an electrical conductivity of 1 S cm^{-1} and poly(ethylene glycol) diglycidyl ether (PEGDE) were purchased from Sigma-Aldrich and stored in a refrigerator. All these chemicals were used as received. The cellulose nanofibrils (CNFs) used in this study were prepared from bleached birch kraft pulp by 2,2,6,6-tetramethylpiperidine-1-oxyl radical (TEMPO)-mediated oxidation followed by mechanical delamination according to an earlier published method.[35] Briefly, 1 g of cellulose fibers was dispersed in 50 ml of deionized water and mixed with a solution containing 16 mg of TEMPO (0.1 mmol g^{-1} fibers) and 100 mg of NaBr (1 mmol g^{-1} fibers). The pH of the slurry was adjusted to 10.0 by the addition of 0.5 M NaOH, whereafter 10 % NaClO (10 mmol g^{-1} fibers) solution was added dropwise within 3 h, and the reaction was allowed to continue for 9 h while the pH of the reaction was kept at 10.5. The TEMPO-oxidized cellulose was precipitated in ethanol and washed thoroughly with deionized water by centrifugation. Thereafter, the oxidized cellulose (1.0 wt%) was defibrillated in a high-pressure homogenizer (AH-100D, ATS Engineering Limited, China) under 1300 bar to yield the TEMPO-oxidized CNF featuring the anionic surface charge of carboxyl groups of 1.4 mmol g^{-1} determined by conductometric titration. The CNFs were used as a 0.69 wt% water dispersion or diluted 2:1 or 1:1 with water and stored in a refrigerator. The mean width and length of the used CNF were 4.8 nm (n=50) and 260 nm (n=50), respectively, giving an aspect ratio of 0.018. Deionized water (resistivity 18 MΩ·cm) was used throughout the work.

2.2. **Preparation of the polymer dispersions for electrospinning.** A CNF/PEO dispersion was first prepared by mixing 0.57 g ml^{-1} (density assumed to 1 g ml^{-1}) of 6 wt% PEO with 0.14 g ml^{-1} CNF with the desired dilution (no dilution, 0.69 wt%; 2:1 dilution, 0.46 wt%; 1:1 dilution 0.35 wt%) for 5 h with a nutating mixer (VWR International). Thereafter, 0.29 ml of PEDOT-PSS

was added to 1 ml of the above dispersion, and mixing was continued for 6 h. Another dispersion was made in a similar manner, but 0.50 g ml^{-1} PEO was mixed with 0.14 g ml^{-1} CNF dispersion, and 0.36 ml of PEDOT-PSS was added to 1 ml of the dispersion. The desired amount of PEGDE (0, 0.36, 0.71, 3.6, 7.1 µl ml^{-1}) was added to the dispersion immediately before electrospinning to limit the reaction in solution. After the addition of PEGDE, the dispersion was mixed for 20 min. The first dispersion was named 2:1:4 (v:v:v, PEDOT-PSS:CNF:PEO), and the second was named 2.5:1:3.5. The dispersions are designated by the amount of PEGDE as /% PEGDE, e.g., a dispersion with 3.6 µl ml^{-1} PEGDE is denoted as 2:1:4/0.36 %.

2.3. **Electrospinning of PEDOT-PSS/CNF/PEO composite fibers.** The as-prepared polymer dispersion was loaded in a 5 ml plastic syringe connected with a blunt tip metallic needle (1.2×40 mm, without bevel, Terumo®). The syringe was placed on an electrospinning setup consisting of a syringe pump (KDS Legato 200 series, KDScientific) and a high-voltage power supply (PS/ER75P04.0GM1, Glassman High Voltage Inc.) in an electrospinning box. A voltage of 20 or 25 kV was applied between the metallic needle and a grounded collector plate located 15 cm from the tip of the needle. The fibers were collected on aluminum foil for SEM, EDXA and FTIR characterization, on ITO (</=10 Ω/□, Präzisions Glas & Optik) glass for cyclic voltammetric characterization and on pieces of microscope slides (1.5 × 1.5 cm) stuck on aluminum foil for AFM and 4-point-probe measurements. A constant pumping rate of 0.5 or 0.6 ml h^{-1} was used for 1 h.

2.4. **Characterization of morphology and elemental composition.** The morphologies of the PEDOT-PSS/CNF/PEO composite nanofibers were studied by scanning electron microscopy (SEM) using a LEO Gemini 1520 instrument with a Thermo Scientific Ultra Dry Silicon Drift

Detector (SDD). The elemental composition was determined by energy dispersive X-ray analysis (EDXA) using the same instrument. The fiber diameter distributions were determined from the SEM images using ImageJ software.

2.5 **Characterization of electroactivity and stability.** Cyclic voltammetry (CV) measurements were performed in a three-electrode electrochemical cell using ITO glass (surface area 1 cm^2) and a glassy carbon rod as the working and counter electrodes, respectively. A double junction Ag | AgCl || 3 M KCl || 3 M KCl was used as the reference electrode (RL-100, Elmetron®). The potential was controlled with an Autolab PGSTAT30 potentiostat using Nova 2.1.3 software. Five potential cycles, the 5^{th} of which was shown, were performed between -0.5 and 0.5 V in 0.1 M KCl electrolyte solution with a scan rate of 20 mV s^{-1}. Prior to all measurements, the electrolyte solution was deaerated with N_2 gas for 15 min, and during the measurements, N_2 was passed over the surface of the solution.

The long-term stability tests of the nanofibers were performed with CV in 0.1 M KCl solution. The measurements were made every 12 h during the first week and once a week afterwards for two months. In between the measurements, the electrodes were kept in 0.1 M KCl solution and were only removed from the solution to place them in the electrochemical cell for the CV measurements. A second set of CV experiments was performed to observe how exposure to water and subsequent drying in air influenced the charging capacity of the nanofibers. Those experiments were carried out for 3 days in the following way: the CV response was measured immediately after exposure to water and 1 h, 1 day, 2 and 3 days after the exposure by letting the fibers dry in air for 1 h before each CV recording.

2.6 **Ex situ FTIR measurements.** The changes in the fiber chemical structure upon contact with water were studied by Fourier transform infrared (FTIR) spectroscopy. The spectra were recorded using a Harrick's VideoMVP single reflection diamond ATR accessory (incidence angle 45°) with a horizontal sampling area of Ø = 500 μm and a built-in pressure applicator. The ATR accessory was attached to a Bruker IFS 66S spectrometer equipped with a DTGS detector. Small pieces of fibers spun on Al foil were tightly pressed against the diamond crystal, and 32 interferograms were recorded with a resolution of 4 cm^{-1}.

2.7. **Determination of the electrical conductivity.** The 4-point probe method was used in a linear configuration with a tip spacing of 1.82 mm to determine the conductivity of the fibrous PEDOT-PSS/CNF/PEO composite mats. The tips were spring-loaded gold needles with a tip curvature corresponding to a circle of 60 μm diameter. The measurements were made on electrospun nanofibers on a nonconducting glass substrate under ambient conditions with a relative humidity of 25.8 % and at 23.0 °C on dry fiber mats after exposure to water. A bias current of 0.1 mA was applied over the composite material with a Keithley® 2400 SourceMeter. The corresponding stable and reproducible voltage value was used for the calculation of the electrical conductivity using finite-size corrections.[36] The thickness of the fibrous mats was determined by carefully cutting the films with a surgical knife, and the height of these narrow cuts (approximately 10-15 μm) was measured with an NTEGRA PRIMA (NT-MDT, Moscow, Russia) atomic force microscopy (AFM) system. AFM was used instead of optical profilometry due to the efficient light absorption of PEDOT-PSS. The AFM images (512 × 512 pixels) were captured in tapping mode under ambient conditions (T = 22 °C, RH% = 45 ± 3) using silicon cantilevers with a nominal tip radius of 8 nm (Model: HQ:NSC14/AI BS) with a scanning rate of 0.20-0.35 Hz. Three 80 × 80 μm images per film were taken from different locations; from each image, 10 lines were analyzed,

and the average thicknesses of the films were calculated. Image analysis was performed using SPIP™ image analysis software (Image Metrology, Lyngby, Denmark).

2.8 **Biocompatibility tests with photosynthetic microbes.** A model microalga, *Chlamydomonas reinhardtii* wild-type strain CC-124 (hereafter, *Chlamydomonas*), was cultured in standard Tris-acetate-phosphate (TAP) medium (pH 7.2).[37] The cells were grown photomixotrophically under continuous white light illumination of 50 μmol photons m^{-2} s^{-1} photosynthetic active radiation (PAR) at 25 °C under agitation on a rotary shaker (120 rpm) at atmospheric CO_2 levels. A model cyanobacterium, *Synechocystis* sp. strain PCC 6803 (hereafter, *Synechocystis*), was cultivated in Blue-Green (BG-11) medium[38] supplemented with 5 mM HEPES NaOH (pH 7.5). The cells were grown photoautotrophically on a rotary shaker (120 rpm) at 30 °C under continuous white light illumination of 35 μmol photons m^{-2} s^{-1} PAR. The cell densities of all cultures were estimated spectrophotometrically at 750 nm (OD_{750}). The photosynthetic cells were harvested by centrifugation, adjusted to OD_{750} = 0.8 in the respective fresh growth medium and subjected to the biocompatibility test. For this purpose, 1 ml of cell suspension was deposited on the PEDOT-PSS/CNF/PEO film (7 mm × 14 mm) placed in a Petri dish. The PEDOT-PSS/CNF/PEO film for this purpose was made with a dispersion composition of 2.5:1:3.5/0.07 % by using 0.69 wt% CNF on an ITO glass substrate, and a 25 kV applied voltage and 0.6 ml h^{-1} feeding rate were used during electrospinning. The cell layer was illuminated from the top with continuous white light of the same intensity as applied during cultivation. To avoid cell drying, 500 μl of the respective growth medium was added to the cells every 24 h. Control cells were prepared similarly on ITO glass, except a PEDOT-PSS/CNF/PEO film was not introduced. Photosynthetic parameters were determined by measuring room temperature

chlorophyll fluorescence directly from the intact cells using a pulse-amplitude modulation fluorimeter (PAM-2000, Walz, Germany). For this purpose, the cells were dark-adapted for 5 min, and the initial chlorophyll fluorescence (F_0) and the maximum fluorescence (F_m) were measured by applying a weak measuring light (2 μmol photons m^{-2} s^{-1}) and a strong saturating pulse (4000 μmol photons m^{-2} s^{-1}, 0.8 s), respectively. After measurements of photosynthetic parameters, the cell layer was brought back to white light illumination from the top side. The maximum quantum efficiency of photosystem II, F_v/F_m, ($F_v/F_m = (F_m - F_0)/F_m$) was calculated as a measure of photosynthesis.[37,38]

3. RESULTS AND DISCUSSION

3.1. **Effects of polymer dispersion composition and electrospinning conditions on fiber morphology.**

In electrospinning, the fiber morphology is heavily reliant on the dispersion parameters such as viscosity, surface charge density, molecular weight and surface tension along with the process parameters including the applied electric field, tip-to-collector distance and feeding rate of the dispersion. In addition to these variables, ambient parameters such as humidity and temperature play a role in determining the fiber morphology and diameter.[1,2] The specific dispersion composition used in this study is the result of extensive optimization work, which is not discussed in detail here. However, the effects of the amounts of CNFs, PEDOT-PSS and PEGDE as well as the applied voltage and the feeding rate of the dispersion during electrospinning on the fiber morphology are thoroughly considered in this research.

Effect of the CNF concentration. To observe how the concentration of CNFs affects the fiber morphology, dispersions with a composition of 2:1:4/0.07 % (PEDOT-PSS:CNF:PEO/% PEGDE) were prepared using CNF dispersions with concentrations of 0.35 wt%, 0.46 wt% or 0.69 wt%. A

dispersion containing no CNFs (2:0:4/0.07 %) was also prepared. These dispersions were electrospun using two sets of electrospinning parameters (20 kV, 0.5 ml h^{-1} and 25 kV, 0.6 ml h^{-1}). Figure 1 shows, in the upper row, that the amount of bead-like structures in the fibers was overall rather low when 20 kV applied voltage and 0.5 ml h^{-1} feeding rate were used during the electrospinning process. On the other hand, a slight decrease in the beadlike structures was noticeable with increasing CNF concentration when 25 kV and 0.6 ml h^{-1} were used (Figure 1, bottom row). The amount of fibers also increased slightly with high CNF loading when using these electrospinning parameters. Generally, more uniform fibers with a smaller fiber diameter and fewer beads are produced by increasing the surface charge density and the concentration of the polymer dispersion. An increase in the applied voltage usually also favors the formation of fibers with narrower diameters. In contrast, an increase in the polymer feeding rate increases the fiber diameter and the probability for beaded fibers.[2] An increase in the concentration of the highly charged CNFs in the polymer dispersion increases the charge density of the solution due to anionic carboxylate groups (1.4 mmol g^{-1}) on the surface of the CNFs. This effect might help electrospinning of beadless fibers or fibers with only a few spindle-like beads. An increase in the CNF concentration in the polymer dispersion, however, required an increase in the applied voltage and the feeding rate during electrospinning. SEM images of the fibers fabricated using 20 kV applied voltage with a lower and higher feeding rate (0.4 ml h^{-1} and 0.6 ml h^{-1}, respectively) are shown in the supporting material (S1). Again, an increase in the CNF concentration and decrease in the feeding rate decreased the amount of bead-like structures in the fibers. However, with a higher applied voltage, an increased feeding rate was required to obtain beadless fibers. Increases in the dispersion concentration, viscosity, surface charge density, applied voltage and feeding rate all contributed to the formation of a large amount of fibers on the aluminum foil. Electrospinning

with a dispersion with no CNFs formed shorter and thicker noncontinuous fibers (Figure 1A) than those electrospun with CNFs in the dispersion. This finding is consistent with the fact that electrospinning a polymer dispersion with a low conductivity forms thick fibers. The lower viscosity of the dispersions without CNFs compared to dispersions with CNFs could also cause the formation of short and thick fibers. On the other hand, PEGDE likely affected the morphology of the fibers without CNFs, as shown in Figure S3. If no CNFs were present, PEGDE appeared to thicken and chop the fibers, but thin, smooth and continuous fibers were formed when no PEGDE was added to the polymer dispersion.

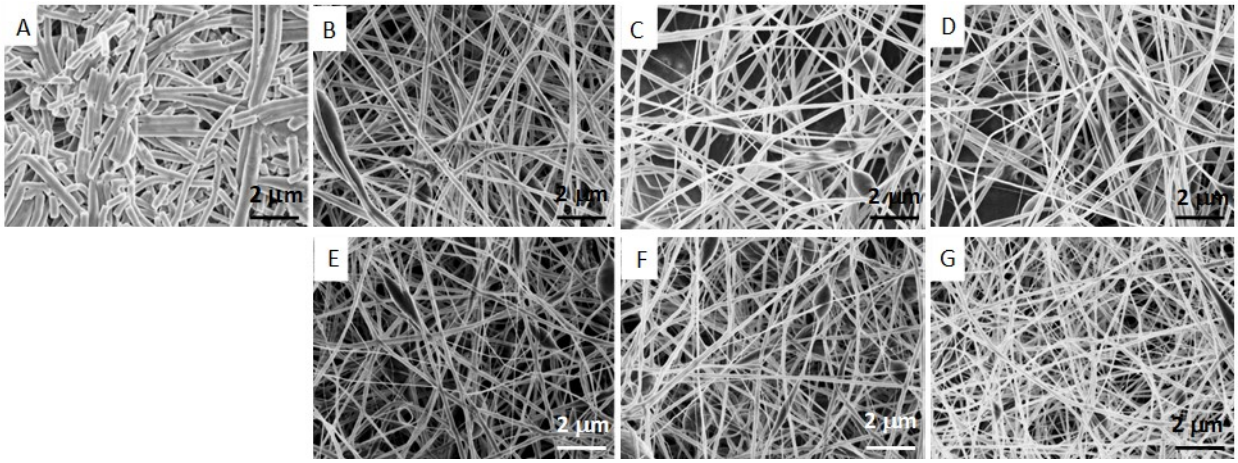

Figure 1. SEM images of PEDOT-PSS/CNF/PEO nanofibers electrospun with a dispersion composition of 2:1:4/0.07 % using (A) no CNFs, (B) 0.35 wt%, (C) 0.46 wt%, (D) 0.69 wt% CNF, 20 kV applied voltage, 0.5 ml h^{-1} feeding rate and (E) 0.35 wt%, (F) 0.46 wt%, (G) 0.69 wt% CNFs with a 25 kV applied voltage and 0.6 ml h^{-1} feeding rate.

Effect of the loading of PEDOT-PSS. The aim of this study was to form fibers for bioelectrochemical applications with high electrical conductivity and charging capacity. Therefore, the effect of an increase in the concentration of the electrically conductive component

PEDOT-PSS in the electrospinning dispersion on the fiber morphology was studied. The PEDOT-PSS loading in the polymer dispersion was increased from 28.6 wt% to 35.7 wt% (PEDOT-PSS:CNF:PEO ratios of 2:1:4 and 2.5:1:3.5, respectively). SEM images of the fibers electrospun with the higher PEDOT-PSS loading with increasing CNF concentration using 20 kV applied voltage and a 0.5 ml h^{-1} feeding rate and of the fibers electrospun using 25 kV applied voltage and a 0.6 ml h^{-1} feeding rate are shown in the Supporting material Figure S4. The fiber morphology with higher PEDOT-PSS loading was highly correlated with the amount of CNFs in the polymer dispersion: excessively low and high amounts of CNFs contributed to distorted fibers. While increasing the applied voltage and feeding rate (Figures S4E and S4F), it was also possible to electrospin uniform fibers with the highest CNF loading using a higher loading of PEDOT-PSS. This finding accounts for the increase in the concentration, surface charge density and viscosity of the polymer dispersion benefiting from a higher applied voltage and feeding rate during electrospinning. The fiber diameter distributions of the fibers made of the polymer dispersion compositions 2:1:4/0.07 % and 2.5:1:3.5/0.07 % using the highest CNF concentration are also shown in Supporting material in Figures S5A and S5B, respectively. The increase in the PEDOT-PSS loading in the polymer dispersion increased the mean diameter of the fibers from 110±40 nm (n=50) to 200±30 nm (n=50). The corresponding SEM images are shown in Figures 1G and S4F, respectively. We believe that the lower viscosity of the dispersion is the reason for the larger fiber diameters.

Effect of the PEGDE loading. The fibrous mats electrospun with a dispersion composed only of hydrophilic polymers generally have poor mechanical strength and tend to disintegrate and dissolve instantaneously when subjected to aqueous solutions.[31] Therefore, a crosslinking strategy using PEGDE was used in this study. PEGDE contains two epoxy groups that can react with amino,

hydroxyl and carboxyl groups. There are many hydroxyl groups in the CNFs and PEO. CNFs also contain carboxyl groups due to oxidation of the $–CH_2OH$ groups of glucose moieties by TEMPO. These carboxyl groups react with the epoxy groups of PEGDE by opening the epoxy rings.[41] We determined the optimum ratios of PEGDE/CNF and PEGDE/PEDOT-PSS in the polymer dispersions, which yielded fibers with the most uniform morphologies. Figure 2 shows, as an example, SEM images of fibers electrospun without PEGDE and with 0.71 % PEGDE in the polymer dispersions using 0.69 wt% CNFs. The 20 kV applied voltage and 0.5 ml h^{-1} feeding rate were used as the electrospinning process parameters for the samples shown in Figures 2A-D, while 25 kV and 0.6 ml h^{-1} were used for the samples in Figures 2E-F. Without PEGDE and with 0.71 % PEGDE in the polymer dispersion, the fibers became distorted and had a glue-like appearance. However, the higher applied voltage and feeding rate also improved the morphology in these cases. Fibers electrospun with increased PEDOT-PSS loading (2.5:1:3.5) in the polymer dispersion are shown in Figures 2C-F; the only difference between Figures C-D and E-F is the process parameters used. Application of the higher voltage and feeding rate improved the fiber morphology when the increased loading of PEDOT-PSS was used. A smoother and more open fiber morphology was then obtained. The optimum loading of PEGDE was, however, found to be 0.07 %. The corresponding SEM images of fibers made with 0.07 % PEGDE while using a 20 kV applied voltage and 0.5 ml h^{-1} feeding rate or 25 kV and 0.6 ml h^{-1} are shown in Figures 1D and S4F, respectively. This same loading of PEGDE was also optimal for lower CNF concentrations (0.46 wt% CNFs) in the polymer dispersion (not shown).

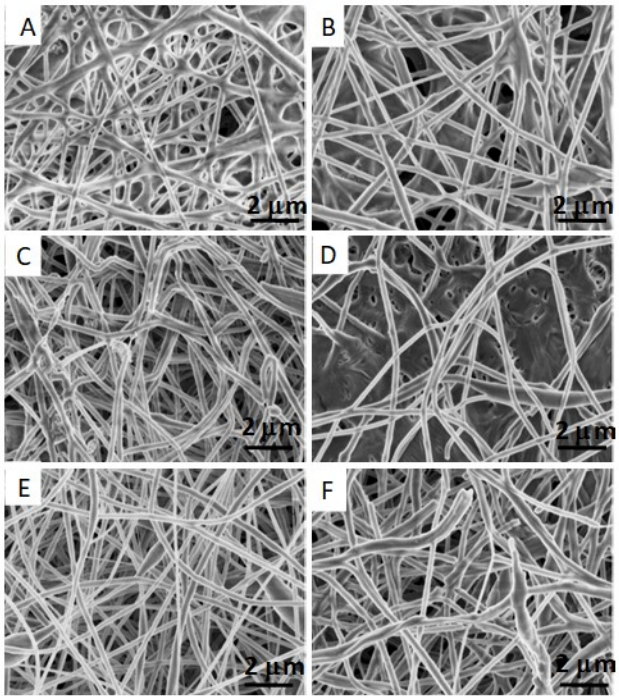

Figure 2. SEM images of PEDOT-PSS/CNF/PEO nanofibers electrospun with different loadings of PEGDE, (A,C,E) no PEGDE, (B,D,F) 0.71 % PEGDE. The dispersion composition of 2:1:4 is shown in (A,B), and 2.5:1:3.5 is shown in (C-F); a 20 kV applied voltage and 0.5 ml h^{-1} feeding rate were used in (A-D) and 25 kV, 0.6 ml h^{-1} in (E-F); 0.69 wt% CNFs was used for all samples.

Effect of water contact. The morphology of the fibrous mats changed after contact with water, as shown in Figure 3. The figure presents typical SEM images of the fibrous mats when the fibers were electrospun with a polymer dispersion composition of 2.5:1:3.5/0.07 % by using the highest CNF concentration, 25 kV applied voltage and 0.6 ml h^{-1} feeding rate and then immersing them in water. After contact with water, some parts of the fibers dissolved, and the mean diameter of the fibers increased from 200±30 nm (n=50) to 360±170 nm (n=50). The fiber diameter distribution when the fibers were in contact with aqueous solution is shown in Figure S5C. The remaining

fibrous mat, however, showed high electrical activity and enhanced stability in aqueous solution, which were further demonstrated by cyclic voltammetry.

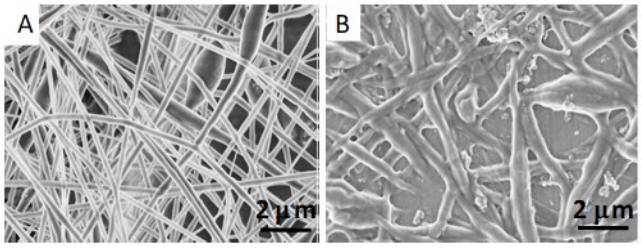

Figure 3. SEM images of PEDOT-PSS/CNF/PEO nanofibers electrospun with dispersion compositions of 2.5:1:3.5/0.07% and 0.69 wt% CNFs, (A) before and (B) after water contact with a 25 kV applied voltage and 0.6 ml h^{-1} feeding rate.

3.2. Study of the electroactivity, stability and electrical conductivity of the electrospun fibrous mats

Effect of the loading of PEDOT:PSS. The electrochemical behavior of PEDOT-PSS in the fibrous mats was characterized by cyclic voltammetry (CV) experiments in 0.1 M KCl aqueous electrolyte solution. Figure 4 shows the CV curves of PEDOT-PSS/CNF/PEO nanofibers electrospun with two different loadings of PEDOT-PSS (2:1:4/0.07 % vs. 2.5:1:3.5/0.07 %) in the electrospinning polymer dispersion. The applied voltage and feeding rate in both cases were 25 kV and 0.6 ml h^{-1}, and 0.69 wt% CNFs was used in the dispersion. As the PEDOT-PSS loading in the polymer dispersion increased from 28.6 wt% to 35.7 wt%, the charging capacity of PEDOT-PSS in the electrospun fibrous mat increased by approximately 88 %. This result is not surprising because after the percolation threshold for the PEDOT concentration in the fibers is exceeded, electron hopping between the PEDOT chains becomes possible, and the electroactivity is increased.

Therefore, all the CV curves discussed hereafter in this section are based on electrospun mats made with a polymer dispersion composition of 2.5:1:3.5, i.e., with 35.7 wt% PEDOT:PSS.

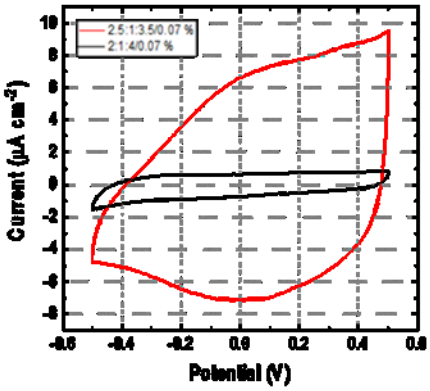

Figure 4. Cyclic voltammograms of PEDOT-PSS/CNF/PEO nanofibers electrospun on ITO glass with dispersion compositions of 2:1:4/0.07 % and 2.5:1:3.5/0.07 % (0.69 wt% CNFs) in 0.1 M KCl using a 20 mV s^{-1} scan rate. A 25 kV applied voltage and 0.6 ml h^{-1} feeding rate were used during electrospinning.

Effect of the loading of PEGDE. The loading of PEGDE in the electrospinning polymer dispersion also had a major effect on the fibers' charging capacity. A tenfold increase in the PEGDE loading in the polymer dispersion, from 0.07 % to 0.7 %, decreased the charging capacity of PEDOT-PSS in the mats by approximately 60 % (Figure S5). The reason for this result could be that the increased crosslinking between the CNFs and PEGDE in the nanofiber structure hindered the hopping of electrons between the PEDOT chains. Another reason could be that the increased crosslinking between PEO and PEGDE prevented PEGDE dissolution and therefore hindered electron movement. The increased crosslinking also induced a morphological difference between the nanofibers with lower and higher loadings of PEGDE, as shown in Figures S4F and 2F, respectively. We found that the fibers turned out to be thicker and were more fused in the fibrous

mats with 0.71 % PEGDE. On the other hand, a five-fold decrease in the PEGDE loading in the polymer dispersion, from 0.07 % to 0.036 %, increased the charging capacity of PEDOT-PSS in the mats by approximately 40 % (Figure S5).

Stability tests. The stability of the fibrous mats in contact with water was next studied over a period of two months. Five consecutive potential cycles were performed in 0.1 M KCl solution for the fibers not in contact with water (0 h), after 1 h and 12 h of contact with water and thereafter every 12 h during the first week, followed by once a week up to two months. The fibrous mats were stored in 0.1 M KCl between the measurements and were transferred to a freshly deaerated solution immediately before the measurement was performed. To account for probable mass variations in the fibrous mats formed during the electrospinning process, the mass of the ITO glass was measured before and after electrospinning to determine the mass of the nanofibers collected on the electrode. Therefore, instead of current density, the current response in the CV curves is given as the current divided by the mass of the original dry fibrous mat. Figures 5A and 5B show the CV results from the long-term stability tests by using different applied voltages, 20 and 25 kV, respectively, and feeding rates, 0.5 and 0.6 ml h^{-1}, respectively, during the electrospinning process. The processing parameters appeared to have a large effect on the fiber stability but not on the initial charging capacity of PEDOT-PSS in the fibers. The fibrous mat electrospun with the higher applied voltage and feeding rate was stable up to 2 months, with even a small increase of 1.7 % in the charging capacity. On the other hand, fibers electrospun with the lower voltage and feeding rate started to lose their electroactivity after 1 h in contact with water, and the overall decrease in charging capacity over 2 months was 32 %.

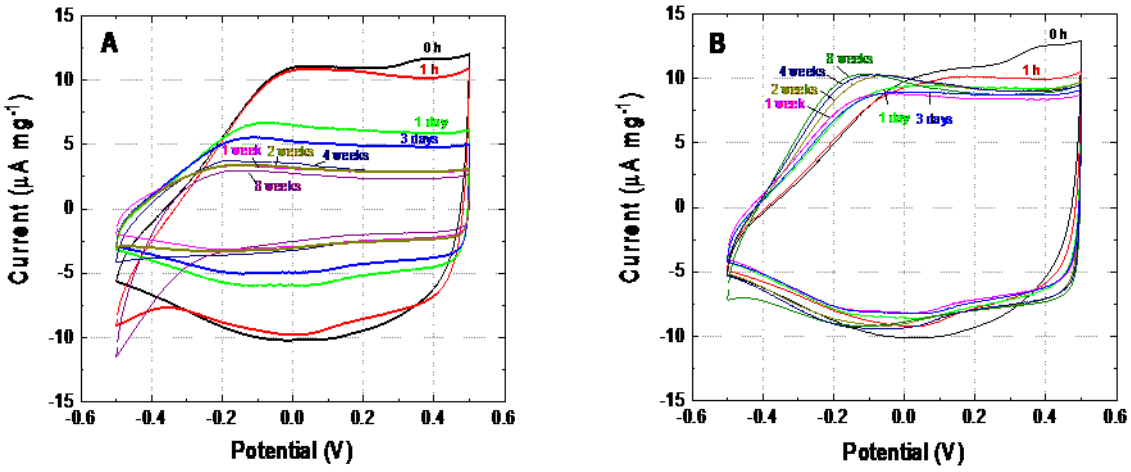

Figure 5. Cyclic voltammograms of PEDOT-PSS/CNF/PEO nanofibers in 0.1 M KCl made with a dispersion composition of 2.5:1:3.5/0.07 % (0.69 wt% CNFs) and electrospun with (A) a 20 kV applied voltage and 0.5 ml h^{-1} feeding rate and (B) a 25 kV applied voltage and 0.6 ml h^{-1} feeding rate. The scan rate was 20 mV s^{-1}.

Effect of the CNF concentration on electroactivity and stability. We studied the effect of the loading of CNFs in the electrospinning polymer dispersion on the electroactivity and stability of the fibrous mats. To do so, we studied the polymer dispersion composition 2.5:1:3.5/0.07 % and used 0.35 or 0.46 wt% CNFs instead of 0.69 wt%. The results are shown in Figure 6. Because the concentration, surface charge density and viscosity of the polymer dispersions decreased when the CNF concentration decreased, we had to lower the applied voltage to 20 kV and decrease the feeding rate to 0.5 ml h^{-1}. In the CV curves, first higher oxidation and reduction currents of PEDOT were obtained when a higher CNF loading was used in the electrospinning polymer dispersion. Second, there was not a large difference if 0.46 wt% or 0.69 wt% CNFs were used. However, after 115 potential cycles and storage in the aqueous electrolyte solution during the experiment (8 weeks), the onset of the oxidation reaction of PEDOT moved to lower potentials for the fibers with

the higher CNF loading than for those with the lower loading. This result indicates that the oxidation of PEDOT became easier with prolonged potential cycling when the fibers included a higher loading of CNFs. Most likely, the higher loading of CNFs in the fibers induced increased swelling of the fibers and made the p-doping reaction of PEDOT easier because of a higher amount of water inside the fiber structure, which facilitated the influx and efflux of doping ions.

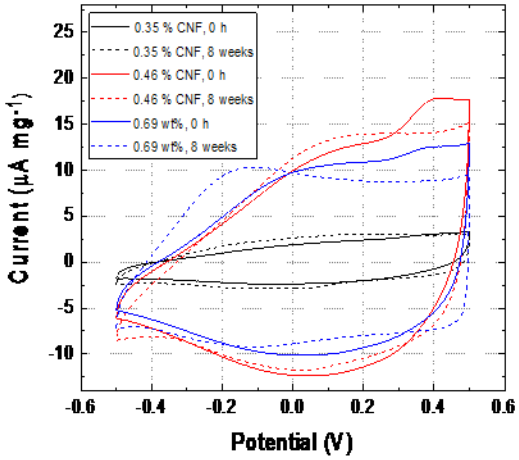

Figure 6. Cyclic voltammograms of PEDOT-PSS/CNF/PEO nanofibers in 0.1 M KCl made with a dispersion composition of 2.5:1:3.5/0.07 % by using 0.35 wt% and 0.46 wt% CNFs (instead of 0.69 wt% CNFs). Electrospun with a 20 kV applied voltage, 0.5 ml h^{-1} feeding rate and 20 mV s^{-1} scan rate.

Effect of drying time. The CV measurements described previously were conducted either with fibers that had never been in contact with water before the experiment or on wet fibers directly after water contact. Next, we studied how the time of incubation of the fibers in water and a subsequent 1 h drying time affected their CV curves. We found that this treatment increased the charging capacity of the fibers compared to fibers with no water contact or wet fibers. This

phenomenon was systematically studied with a few fiber compositions made with different loadings of CNFs and PEGDE in the electrospinning polymer dispersion on the same fiber mat that had not been in contact with water (0 h) and after 1 h, 24 h, 48 h and 72 h of contact with water. Figure 7 shows the CV results for dry fibers after 0 and 72 h of water treatment. The CV responses after 1, 24 and 48 h were between the responses after 0 and 72 h of water treatment and are not shown for simplicity. The resulting charging capacities of all fiber mats increased after the water treatment and subsequent drying period compared to that of the same fiber mats without similar treatment. For example, the charging capacity of PEDOT-PSS/CNF/PEO nanofibers with a composition of 2.5:1:3.5/0.07 % made by using 0.35 wt% CNFs did not increase even after a 56-day water treatment period without a 1 h drying period before recording the CV curves (black curve in Figure 6). On the other hand, a 3-day water treatment period with a subsequent 1 h of drying before CV analysis was enough to increase the charging capacity by approximately 20 % (blue curves in Figure 7). Moreover, the charging capacity of the nanofiber mats made with an electrospinning polymer dispersion with a higher loading of CNFs (0.69 wt%) and a lower loading of PEGDE (0.036 %) (red curves in Figure 7) was high even before the water treatment and subsequent drying but could still be increased by 60 % when introducing a drying period. The reason for this phenomenon is difficult to explain, but reorganization of the chain-like structure in conducting polymer films during continuous potential cycling is a well-known phenomenon.[42] A more crystalline than amorphous structure of conducting polymer films usually also gives rise to a higher charging capacity and electrical conductivity.[43] It can be speculated that the polymer chain structure in the nanofiber mats rearranges during potential cycling and exposure to electrolyte salt solution and continues to reorganize during the drying period as a result of the crystallization process of both PEO and PEDOT:PSS. A combination of all these phenomena is a more likely

reason for the increased charging capacity than only reorganization of PEDOT:PSS during cycling. O. Inganäs and S. Ghosh[44] have shown that a blend of PEDOT-PSS with PEO gives a higher charging capacity than that of pure PEDOT-PSS. The authors explain that this result is due to the high ionic conductivity of PEO and because the swollen morphology of the polymer allows high mobility of the electrolyte ions. Another explanation is that excess dopant ions within the PEDOT-PSS structure are expelled during potential cycling and contact with the electrolyte salt solution (0.1 M KCl), therefore making the redox reaction of PEDOT easier. This effect alone cannot explain the increased charging capacity in this case because it could also have happened during the stability tests without drying before potential cycling. Therefore, during the subsequent drying period, the crystallization process must have continued to reorganize the polymer structure.

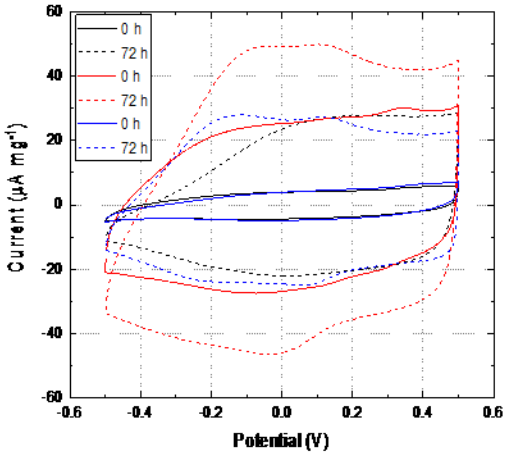

Figure 7. Cyclic voltammograms in 0.1 M KCl of dry PEDOT-PSS/CNF/PEO nanofibers made with dispersion compositions of 2.5:1:3.5/0.36 % (black curves) and 0.036 % (red curves) by using 0.69 wt% CNFs and 2.5:1:3.5/0.07 % (blue curves) by using 0.35 wt% CNFs after 0 and 72 h of water treatment. Electrospun with a 25 kV applied voltage, 0.6 ml h^{-1} feeding rate and 20 mV s^{-1} scan rate.

Electrical conductivity. The electrical conductivity of electrospun mats is of utmost importance for their further use in various applications. Therefore, the electrical conductivity of the PEDOT-PSS/CNF/PEO electrospun mat prepared with the optimum composition of 2.5:1:3.5/0.07 % in the electrospinning polymer dispersion was determined by the 4-point probe method. Two films with different thicknesses of 1.0 ± 0.3 μm and 3.3 ± 0.5 μm were used for the measurements, and they showed a mean electrical conductivity of 13 ± 5 S m^{-1}. This value is considered to be suitable for the further use of these nanofibrous mats in bioelectrochemical applications.

3.3. FTIR-ATR study of the electrospun fibrous mats. As shown in the SEM images of the nanofiber mats in Figure 3, some parts of the fiber structure dissolved upon water contact, and the fiber diameter increased from approximately 200 to 360 nm. The changes in the fiber structure after water contact were investigated by FTIR-ATR measurements. The spectra of the nanofibrous mats before and after water contact are compared to the spectra of PEO, PEDOT-PSS and the CNFs in Figure 8. The intense bands at approximately 1092 and 841 cm^{-1} in the spectrum of PEO (green line in Figure 10) assigned to C-C-O stretching vibrations[45a] and at 953 cm^{-1} to assigned CH_2 twisting vibrations in $–CH_2$-OH[45a] are highly visible in the spectrum of the nanofibrous mats before water contact (black line in Figure 8). After water contact, the vibrations of these groups in the spectrum of the nanofibrous mat (blue line in Figure 8) are no longer as visible, and rather, the spectrum starts to resemble that of PEDOT-PSS (red line in Figure 8) and the CNFs (purple line in Figure 8). Vibrations between 1519 and 1290 cm^{-1} due to C-C (quinoid) and C=C (benzoic) structures in the thiophene ring[46,47] and at 1185, 1127 and 1077 cm^{-1} due to C-O-C bond stretching and the weak vibration at 1050 cm^{-1} due to C-O stretching in the ethylenedioxy group in the PEDOT structure[46,47] are all highly noticeable in the spectrum of the nanofiber mat after water contact. In addition, the bands at 966, 926 and 826 cm^{-1} assigned to C-S bond stretching[46] in

PEDOT are highly visible in the spectrum of the nanofiber mat after water contact. The broad and intense band in the spectrum of the CNFs between 1190 and 870 cm^{-1} with a maximum at 1030 cm^{-1} assigned to C-O[48] and C-O-C[48,49] stretching vibrations and the bands at 1600 and 1416 cm^{-1} assigned to OH deformation vibration[45b] and to CH_2 deformation vibration[45b], respectively, are also visible in the spectrum of the nanofiber mat after water contact. All these FTIR bands verify the presence of PEDOT-PSS as well as CNFs and the disappearance of some part of the PEO in the nanofiber mats after water contact. On the other hand, the existence of the bands at 951 and 834 cm^{-1} in the nanofibers after water contact verifies that not all PEO dissolved during the water contact. These findings verify that the cross-linking reaction mainly occurred between the hydroxyl and carboxyl groups of CNF and the epoxy groups of PEGDE. Due to the high molecular weight of PEO (Mv 600 000 g mol^{-1}) there exists only a few free hydroxyl groups at the end of its polymeric chains capable of reacting with the epoxy groups of PEGDE.

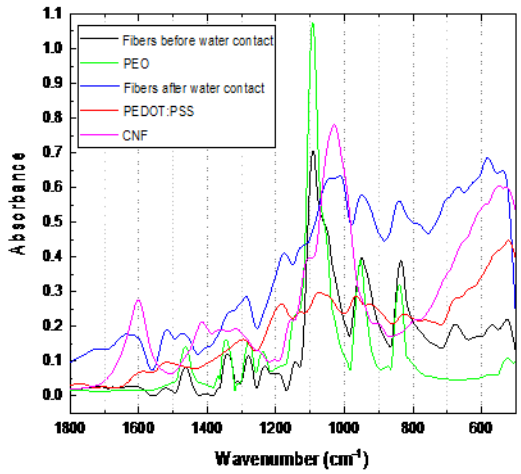

Figure 8. FTIR-ATR spectra of PEDOT-PSS/CNF/PEO nanofibers prepared with a dispersion composition of 2.5:1:3.5/0.07 % on Al foil before water contact (–) and after water contact (–) and

the spectra of PEO (–), PEDOT-PSS (–) and the CNFs (–). The fibers were electrospun with a 25 kV applied voltage and 0.6 ml h^{-1} feeding rate.

3.4 **Energy Dispersive X-ray Analysis.** Table 1 shows the energy dispersive X-ray analysis results and the C/S ratio in the fibrous mats made with a dispersion composition of 2.5:1:3.5/0.07 % before and after water contact and with two different processing parameters. Because only PEDOT-PSS contains sulfur in its chemical structure, the lower C/S ratio after water contact confirms that some parts of PEO in the fibers rather than PEDOT dissolve during water contact, as already indicated by the FTIR results. The C/S content in the fibrous mat electrospun with a 25 kV applied voltage and 0.6 ml h^{-1} feeding rate is lower than that in the mat made with 20 kV and 0.5 ml h^{-1}. This result indicates that it was possible to load more PEDOT-PSS into the mats by using the higher processing conditions (higher values of applied voltage and feeding rate). The reason for this is that the molecular mass and viscosity of PEDOT:PSS is much lower compared to PEO and therefore it requires a higher electrospinning voltage and feeding rate in order to be incorporated into the fibrous mats. This finding, on the other hand, can explain the decrease in the electroactivity during prolonged water contact of the mats made with the lower value processing parameters shown earlier in Figure 5. As the FTIR results already indicated, some parts of PEO in the fibers dissolve during contact with water; therefore, the dissolution grade in the fibrous mats made with the lower processing conditions, which most likely include more PEO, is also higher, leading to decreased electroactivity over time.

Table 1. Energy dispersive X-ray analysis results of the fibrous mats.

Polymer dispersion composition	Applied voltage, kV	Feeding rate, ml h^{-1}	Atom concentration, %			C/S ratio	Water contact
			C	O	S		
2.5:1:3.5/0.07 %	25	0.6	59.8	36.8	0.7	85.4	No
2.5:1:3.5/0.07 %	25	0.6	50.3	16.5	1.1	46.2	Yes
2.5:1:3.5/0.07 %	20	0.5	62.3	25.3	0.3	188.8	No

*0.69 wt% CNF was used in the polymer dispersion

3.5 **Biocompatibility of microalgae and cyanobacteria with PEDOT-PSS/CNF/PEO fibrous mats.** To evaluate the biocompatibility of PEDOT-PSS/CNF/PEO fibrous mats made with a dispersion composition of 2.5:1:3.5/0.07 % with photosynthetic microbes, *Chlamydomonas* and *Synechocystis* cells were deposited on the fibrous mat, thus allowing direct contact of the material with the cells (for more details, see the Experimental Section). The fitness of the *Chlamydomonas* and *Synechocystis* cells interacting with PEDOT-PSS/CNF/PEO films was evaluated in the long-term (72 h) experiment as the change in the maximum quantum efficiency of photosystem II (F_v/F_m). In the healthy suspension cultures, the F_v/F_m parameter ranged between 0.7-0.8 in green algae and 0.4-0.5 in cyanobacteria. This value strongly decreases under stress conditions due to inhibition of photosystem II. Figure 9 demonstrates that green algae and cyanobacteria deposited on the PEDOT-PSS/CNF/PEO film maintained the maximum quantum efficiency of photosystem II (F_v/F_m), similar to that of the control cells (deposited on ITO glass without PEDOT-PSS/CNF/PEO) for the duration of the experiment (72 h). In contrast to green algae, the cyanobacterial cells showed a slight decrease in F_v/F_m (0.38) at 72 h. Since this decrease was also monitored in the control cells, we cannot link it to a toxic effect of PEDOT-PSS/CNF/PEO. The results obtained here indicate that the electrospun thin PEDOT-PSS/CNF/PEO films exhibit good biocompatibility and low cytotoxicity toward microalgae and cyanobacteria upon adaptation, making them useful for applications in photobioelectrochemical devices.

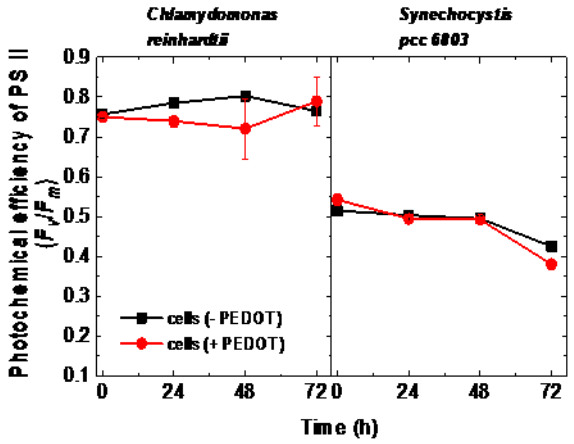

Figure 9. Photosynthetic activity of green algae *Chlamydomonas reinhardtii* and cyanobacterium *Synechocystis* sp. PCC 6803 deposited on PEDOT-PSS/CNF/PEO films made with a dispersion composition of 2.5:1:3.5/0.07 % on ITO glass. The photosynthetic activity was monitored as the maximum quantum efficiency of photosystem II (F_v/F_m). Error bars correspond to the means of standard deviation values derived from two independent biological replicates.

4. CONCLUSIONS

Electrically conductive composite nanofibers of PEDOT-PSS, CNFs and PEO were fabricated from a fully aqueous-based polymer dispersion via the electrospinning technique. It was found that increasing the CNF concentration led to an increase in the polymer dispersion concentration, viscosity and surface charge density and enhanced the electrospinnability of the dispersion, resulting in the formation of a large amount of beadless fibers. In the same way, after an increase in the PEDOT-PSS concentration, the electrospinnability of the polymer dispersion benefited from a higher concentration of CNFs. In both cases, however, an increased applied voltage and feeding rate during electrospinning were required. It was also noted that the electrospinnability benefited from a higher applied voltage and feeding rate after incorporation of the crosslinking agent PEGDE

into the polymer dispersion. The charging capacity of the fibrous mats could be increased by approximately 88 % by increasing the loading of PEDOT-PSS in the polymer dispersion from 29 to 36 wt%. The increase in the charging capacity, however, was highly dependent on the amount of PEGDE loaded in the original polymer dispersion. The fibrous mats showed stable electroactivity in aqueous electrolyte solution during at least the two-month measurement period despite some portion of PEO (regardless of the crosslinking) dissolving during water contact, as demonstrated by the FTIR measurements. The cyclic voltammetric behavior of the fibrous mats also showed that a higher loading of CNFs in the fibers induced an increased swelling of the fibers and facilitated the p-doping of PEDOT. The charging capacity could also be increased up to 60 % by drying the fibrous mats after water contact. The latter effect was a result of the swelling and subsequent crystallization of the fibers, enhancing the movement of electrons and ions in the fibrous mats. The electrical conductivity of the PEDOT-PSS/CNF/PEO fibrous mats measured by the 4-point probe method was found to be 13 ± 5 S m^{-1}. Finally, the photosynthetic capability of microalgae and cyanobacteria on the electroconductive fibrous mats was preserved, indicating the good biocompatibility and low cytotoxicity of these mats and their suitability for further studies in photosynthetic bioelectrochemical cells.

ASSOCIATED CONTENT

Supporting Information. – TEM image of the cellulose nanofibrils (Figure S1)

- Additional SEM images of PEDOT-PSS/CNF/PEO nanofibers clarifying the differences in the polymer dispersion composition on the nanofiber morphology: effect of the feeding rate with different CNF loadings (Figure S2) and the effect of PEGDE loading when no CNFs are present

in the polymer dispersion (Figure S3). SEM images showing the effect of the processing parameters: applied voltage and feeding rate to fibers with different load of CNF (Figure S4).

- Fiber diameter distributions of PEDOT-PSS/CNF/PEO nanofibers electrospun with different dispersion compositions (Figure S5).

- Cyclic voltammograms of PEDOT-PSS/CNF/PEO nanofibers with different loadings of PEGDE (Figure S6).

This material is available free of charge via the Internet at http://pubs.acs.org.

AUTHOR INFORMATION

Corresponding Author

***E-mail:** rose-marie.latonen@abo.fi

ORCID

Rose-Marie Latonen: 0000-0002-8378-0991

Zhanna Boeva: 0000-0003-4801-4519

Sergey Kosourov: 0000-0003-4025-8041

Xiaoju Wang: 0000-0002-1728-4164

Chunlin Xu: 0000-0003-1860-9669

Yagut Allahverdiyeva: 0000-0002-9262-1757

Author Contributions

The manuscript was written through contributions of all authors. / All authors have given approval to the final version of the manuscript. / ‡, § These authors contributed equally.

Funding Sources

The work of Xu C. and Wang X. was supported by the Academy of Finland (project#298325). Zhanna Boeva is grateful to the Jane and Aatos Erkko Foundation for financial support. This work was also supported by the Novo Nordisk Fonden (project #NNF16OC0021626) and SmartBio Biocity Turku Research Program.

ACKNOWLEDGMENT

The authors wish to express their appreciation to Linus Silvander (Åbo Akademi University) for performing the SEM measurements.

ABBREVIATIONS

AFM, atomic force microscopy; BG-11, Blue-Green medium; CNCs, cellulose nanocrystals; CNFs, cellulose nanofibrils; CV, cyclic voltammetry; ECPs, electrically conducting polymers; EDXA, energy dispersive X-ray analysis; F_0, initial chlorophyll fluorescence; F_m, maximum chlorophyll fluorescence; F_v/F_m, maximum quantum efficiency of photosystem II; FTIR-ATR, Fourier transform infrared attenuated total reflectance; PAR, photosynthetic active radiation; PEDOT-PSS, poly(3,4-ethylenedioxythiophene) doped with poly(styrenesulfonate); PEGDE, poly(ethylene glycol) diglycidyl ether; PEO, poly(ethylene oxide); PLA, poly(lactic acid); PVA, poly(vinyl alcohol); SDD, silicon drift detector; SEM, scanning electron microscopy; TAP, Tris-acetate-phosphate; TEMPO, 2,2,6,6-tetramethylpiperidine-1-oxyl radical

REFERENCES

(1) Tebyetekerwa, M.; Ramakrishna, S. What is next for electrospinning? *Matter* **2020**. 2, 279.

(2) Bhardwaj, N.; Kundu, S. C. Electrospinning: A fascinating fiber fabrication technique. *Biotechnol. Adv.* **2010**, 28, 325-347.

(3) Park, W.-I.; Kang, M.; Kim, H.-S.; Jin, H.-J. Electrospinning of poly(ethylene oxide) with bacterial cellulose whiskers. *Macromol. Symp.* **2007**, 247-250, 289-294.

(4) Han, J.; Wang, S.; Zhu, S.; Huang, C.; Yue, Y.; Mei, C.; Xu, X.; Xia, C. Electrospun core-shell nanofibrous membranes with nanocellulose-stabilized carbon nanotubes for use as high-performance flexible supercapacitor electrodes with enhanced water resistance, thermal stability, and mechanical toughness. *ACS Appl. Mater. Interfaces* **2019**, 11, 44624-44635.

(5) Wang, H.; Kong, L.; Ziegler, G. R. Fabrication of starch – nanocellulose composite fibers by elctrospinning. *Food Hydrocolloids* **2019**, 90, 90-98.

(6) Si, J.; Cui, Z.; Wang, Q.; Liu, Q.; Liu, C. Biomimetic composite scaffolds based on mineralization of hydroxyapatite on electrospun poly(*ε*-caprolactone)/nanocellulose fibers. *Carbohyd. Polym.* **2016**, 143, 270-278.

(7) Martínez-Sanz, M.; Lopez-Rubio, A.; Villano, M.; Oliveira, C. S. S.; Majone, M.; Reis, M.; Lagarón, J. M. Production of bacterial nanobiocomposites of polyhydroxyalkanoates derived from waste and bacterial nanocellulose by the electrospinning enabling melt compounding method. *J. Appl. Polym. Sci.* **2016**, 42486, 1-14.

(8) Esmaeilzadeh, I.; Mottaghitalab, V.; Tousifar, B.; Afzali, A.; Lamani, M. A feasibility study on semi industrial nozzleless electrospinning of cellulose nanofiber. *Int. J. Ind. Chem.* **2015**, 6, 193-211.

(9) Sytka, A.; Sutka, A.; Gaidukov, S.; Timusk, M.; Gravitis, J.; Kukle, S. Enhanced stability of PVA electrospun fibers in water by adding cellulose nanocrystals. *Holzforschung* **2015**, 69, 737-743.

(10) Choi, J.; Park, D. W.; Shim, S. E. Electrospun PEDOT:PSS/carbon nanotubes/PVP nanofibers as chemiresistors for aromatic volatile organic compounds. *Synth. Met*. **2012**, 162, 1513-1518.

(11) Wang, T.; Zhang, Y.; Liu, Q.; Cheng, W.; Wang, X.; Pan. L.; Xu, B.; Xu, H. A self-healable, highly stretchable, and solution processable conductive polymer composite for ul-trasensitive strain and pressure sensing. *Avd. Funct. Mater.* **2018**, 28, 1705551-1705563.

(12) Simsek, M.; von Kruechten, L.; Buchner, M.; Duerkop, A.; Baeumner, A. J.; Wongkaew, N. An efficient post-doping strategy creating electrospun conductive nanofibers with multi-functionalities for biomedical applications. *J. Mater. Chem. C* **2019**, 7, 9316-9325.

(13) Smirnov, M. A.; Tarasova, E. V.; Vorobiov, V. K.; Ka-satkin, I. A.; Mikli, V.; Sokolova, M. P.; Bobrova, N. V.; Vessiljeva, V.; Krumme, A.; Yakimanskiy, A. V. Electroconductive fibrous mat prepared by electrospinning of polyacrylamide-g-polyaniline copolymers as electrode material for supercapacitors. *J. Mater. Sci.* **2019**, *54*, 4859-4873.

(14) Chan, E. W. C.; Bennet, D.; Baek, P.; Barker, D.; Kim, S.; Travas-Sejdic, J. Electrospun polythiophene phenylenes for tissue engineering. *Biomacromolecules* **2018**, *19*, 1456-1468.

(15) Park, E.-S.; Jang, D.-H.; Lee, Y.-I.; Jung, C. W.; woo Lim, D.; Kim, B. S.; Jeong, Y.-K.; Myung, N. V.; Choa, Y.-H. Fabrication and sensing property for conducting polymer

nanowire-based biosensor for detection of immunoglobulin G. *Res. Chem. Intermed.* **2014**, 40, 2565-2570.

(16) Groenendaal, L. B.; Jonas, F.; Freitag, D.; Pielartzik, H.; Reynolds, J. R. Poly(3,4-ethylenedioxythiophene) and its derivatives: Past, present, and future. *Adv. Mater.* **2000**,*12*, 481-494.

(17) Zarrin, N.; Tavanai, H.; Abdolmaleki, A.; Bazarganipour, M.; Alihosseini, F. An investigation on the fabrication of conductive polyethylene dioxythiophene (PEDOT) nanofibers through electrospinning. *Synth. Met.* **2018**, *244*, 143-149.

(18) Bhatnagar, M. P.; Kelkar, S.; Mahanwar, P. Sunthesis and characterization of poly(3,4-ethylenedioxythiophene)/poly(lactic acid) nanofibers by electrospinning. *Polym. Int.* **2017**, *66*, 359-365.

(19) Laforgue, A. All-textile flexible supercapacitors using electrospun poly(3,4-ethylenedioxythiophene) nanofibers. *J. Power Sources* **2011**, *196*, 559-564.

(20) Bolin, M. H.; Svennersten, K.; Wang, X.; Chronakis, I. S.; Richter-Dahlfors, A.; Jager, E. W. H.; Berggren, M. *Sensor Actuator B* **2009**, *142*, 451-456.

(21) Rosario, A.; Pinto, N. J. PEDOT-PSS nanoribbon and cast film field effect transistors with ferroelectric gating. *Synth. Met.* **2019**, *247*, 151-156.

(22) Zhang, Q.; Wang, X.; Fu, J.; Liu, R.; He, H.; Ma, J.; Yu, M.; Ramakrishna, S.; Long, Y. Electrospinning of ultrafine conducting polymer composite nanofibers with diameter less than 70 nm as high sensitive gas sensor. *Materials* **2018**, *11*, 1744, 1-10.

(23) Zhang, H.-D.; Yan, X.; Zhang, Z.-H.; Yu, G.-F.; Han, W.-P.; Zhang, J.-C.; Long, Y.Z. Electrospun PEDOT:PSS/PVP nanofibers for CO gas sensing with quartz crystal microbalance technique. *Int. J. Pol. Sci.* **2016**, ID 3021353, 1-6.

(24) Pinto, N. J.; Rivera, D.; Melendez, A.; Ramos, I.; Lim, J. H.; Johnson, A. T. C. Electrical response of electrospun PEDOT-PSSA nanofibers to organic and inorganic gases. *Sensor Actuator B* **2011**, *156*, 849-853.

(25) Choi, J.; Lee, J.; Choi, J.; Jung, D.; Shim, S. E. Electrospun PEDOT:PSS/PVP nanofiber as the resistor in chemical vapour sensing. *Synth. Met.* **2010**, *160*, 1415-1421.

(26) Huang, S.-R.; Lin, K.-F.; Don, T.-M.; Lee, C.-F.; Wang, M.-S.; Chiu, W.-Y. Thermoresistive conductive polymer composite thin film and fiber mat: Crosslinked PEDOT:PSS and P(NIPAAm-*co*-NMA) composite. *J. Polym. Sci. Pol. Chem.* **2016**, *54*, 1078-1087.

(27) Bessaire, B.; Mathieu, M.; Salles, V.; Yeghoyan, T.; Celle, C.; Simonato, J.-P.; Brioude, A. Synthesis of continuous conductive PEDOT:PSS nanofibers by electrospinning: A conformal coating for optoelectronics. *ACS Appl. Mater. Interfaces* **2017**, *9*, 950-957.

(28) Tsai, N.-C.; She, J.-W.; Wu, J.-G.; Chen, P.; Hsiao, Y.-S.; Yu, J. Poly(3,4-ethylenedioxythiophene) polymer composite bioelectrodes with designed chemical and

topographical cues to manipulate the behavior of PC12 neuronal cells. *Adv. Mater. Interfaces* **2019**, *6*, 1801576.

(29) Choi, G. M.; Lim,S.-M.; Lee,Y.-Y.; Yi, S.-M.; Lee, Y.-J.; Sun, J.-Y.; Joo, Y.-C. PEDOT:PSS/Polyacrylamide nanoweb: Highly reliable soft conductors with swelling resistance. *ACS Appl. Mater. Interfaces* **2019**, *11*, 10099-10107.

(30) Liu, D.; Yuan, X.; Bhattacharyya, D. The effects of cellulose nanowhiskers on electrospun poly (lactic acid) nanofibers. *J. Mater. Chem.* **2012**, *47*, 3159-3165.

(31) Aqil, A.; Tchemtchoua, V. T.; Colige, A.; Atanasova, G.; Poumay, Y.; Jerôme, C. Preparation and characterization of EGDE crosslinked chitosan electrospun membranes. *Clin. Hemorheol. Microcirc.* **2015**, *60*, 39-50.

(32) Abedi, A.; Hasanzadeh, M.; Tayebi, L. Conductive nanofibrous Chitosan/PEDOT:PSS tissue engineering scaffolds. *Mater. Chem. Phys.* **2019**, *237*, 121882.

(33) Liu, J.; Cheng, F.; Grénman, H.; Spoljaric, S.; Seppälä, J.; Eriksson, J. E.; Willför, S.; Xu, C. Development of nanocellulose scaffolds with tunable structures to support 3D cell culture *Carbohydr. Polym.* **2016**, *148*, 259-271.

(34) Xu, C.; Zhang Molino, B.; Wang, X.; Cheng, F.; Xu, W.; Molino, P.; Bacher, M.; Su, D.; Rosenau, T.; Willför, S.; Wallace, G. 3D printing of nanocellulose hydrogel scaffolds with tunable mechanical strength towards wound healing application *J. Mater. Chem. B* **2018**, *6*, 7066-7075.

(35) Liu, J.; Korpinen, R.; Mikkonen, K. S.; Willför, S.; Xu, C. Nanofibrillated cellulose originated from birch sawdust after sequential extractions: a promising polymeric material from waste to films. *Cellulose* **2014**, *21*, 2587-2598.

(36) Smits, F. M. Measurement of Sheet Resistivities with the Four-Point Probe. *Bell Systems Technical Journal* **1958**, 37, 711-718.

(37) Harris, E. H. The Chlamydomonas source book: a comprehensive guide to biology and laboratory use. Academic Press: San Diego, 1989.

(38) Rippka, R.; Deruelles, J.; Waterbury, J. B.; Herdman, M.; Stanier, R. Y. Generic assignments, strain histories and properties of pure cultures of cyanobacteria. *J. Gen. Microbiol.* **1979**, *111*, 1-61.

(39) Baker, R. Chlorophyll fluorescence: a probe of photosynthesis in vivo, *Annu. Rev. Plant Biol*. **2008**, 59, 89-113.

(40) Touloupakis, B.; Cicchi, G.; Torzillo, A. Bioenergetic assessment of photosynthetic growth of Synechocystis sp. PCC 6803 in continuous cultures. *Biotechnol. Biofuels.* **2015**, *8*,133.

(41) Vasylieva, N.; Barnych, B.; Meiller, A.; Maucler, C.; Pollegioni, L.; Lin, J.-S.; Barbier, D.; Marinesco, S. Covalent enzyme immobilization by poly(ethylene glycol)diglycidyl ether (PEGDE) for microelectrode biosensor preparation. *Biosens. Bioelectron.* **2011**, *26*, 3993-4000.

(42) Kankare, J. Electronically conducting polymers: Basic methods of synthesis and characterization. In Electrical and optical polymer systems, Wise, D. L.; Wnek, G. E.; Trantolo, D. J.; Cooper, T. M.; Gresser, J. D., Eds.; Marcel Dekker, Inc.: New York, 1998; 167-199.

(43) Kim, N.; Kee, S.; Lee, S. H.; Lee B. H.; Kahng, Y. H.; Jo, Y.-R.; Kim, B.-J.; Lee, K. Highly conductive PEDOT:PSS nanofibrils induced by solution-processed crystallization. *Adv. Mater.* **2014**, *26*, 2268-2272.

(44) Ghosh, S.; Inganäs, O. Networks of electron-conducting polymer in matrices of ion-conducting polymers. *Electrochem. Solid St.* **2000**, *3*, 213-215.

(45) Socrates, G. *Infrared and Raman Characteristic Group Frequencies, Tables and Charts* 3rd Ed., John Wiley & Sons, Ltd: Chichester, 2001; (a) Table 6.3, (b) Table 23.3.

(46) Nagarajan, S.; Kumar, J.; Bruno, F. F.; Samuelson, L. A.; Nagarajan, R. Biocatalytically synthesized poly(3,4-ethylenedioxythiophene). *Macromolecules*, **2008**, *41*, 3049-3052.

(47) Dai, C.-A.; Chang, C.-J.; Chi, H.-Y.; Chien, H.-T.; Su, W.-F., Chiu, W.-Y. Emulsion synthesis of nanoparticles containing PEDOT using conducting polymeric surfactant: Synergy for colloid stability and intercalation doping. *J. Polym. Sci., Part A: Polym. Chem.*, **2008**, *46*, 2536-2548.

(48) Zhang, D.; Zhang, Q; Gao, X.; Piao, G. A Nanocellulose polypyrrole composite based on tunicate cellulose. *Int. J. Polym. Sci.*, **2013**, ID 175609, 1-6.

(49) Luong, N. D.; Korhonen, J. T.; Soininen, A J.; Ruokolainen, J.; Johansson, L.-S.; Seppälä, J. Processable polyaniline suspensions through in situ polymerization onto nanocellulose. *Eur. Polym. J.*, **2013**, *49*, 335-344.

Table Of Contents graphic